

Adjustable Gap Rheometry for the Rheological Characterization of Energetic Formulations*

[Dilhan Kalyon](#)¹, Halil Gevgilili¹, James E. Kowalczyk², Suzanne Prickett³ and Constance

Murphy³

(1) Stevens Institute of Technology, Castle Point St., Hoboken, NJ 07030

(2) Material Processing & Research, Inc., 31 Mercer St. 2-E, Hackensack, NJ 07601,

(3) Naval Surface Warfare Center, Indian Head Division, Indian Head, MD 20640-5035

It is difficult to characterize the rheological behavior of energetic suspensions due to their viscoplasticity and wall slip. The use of the rectangular slit geometry, as an on-line or off-line rheometer is advantageous provided that the surface to volume ratio of the slit die can be systematically varied to allow the wall slip corrections to be made. Here two rectangular slit rheometers designed and built to handle the rheological behavior of energetic suspensions are presented. The gap of these rheometers is variable to give the user the ability to vary the gap and the flow rate independently and hence obtain the wall shear stress as a function of the surface to volume ratio of the rheometer, thus enabling wall slip corrections to be made and the slip velocity behavior and the shear viscosity versus the deformation rate material function to be characterized. The slit rheometers rely on a series of pressure transducers, installed flush with the wall, which are used to determine the pressure drop over the fully-developed flow region and hence the wall shear stress directly from the fully developed pressure gradient. The ability to independently vary the mass flow rate and the gap opening allows one to carry-out the wall slip corrections and hence obtain the wall slip velocity versus the shear stress data, which can then be used as the boundary condition during the simulation of the die and extrusion flows and at the same time allow the determination of accurate shear viscosity data. A set of data systematically collected with an on-line slit rheometer with a continuously adjustable gap to characterize the wall slip velocity as well as the shear viscosity material function of a LOVA formulation as a function of deformation rate, solvent concentration and temperature is used to illustrate the working principles of the on-line and off-line adjustable-gap rheometers.

* *The full manuscript is to be published in Journal of Energetic Materials*

I. Introduction

The characterization of the shear viscosity and the wall slip behavior of energetic suspensions requires specialized characterization methods, which not only need to be explosion proof, but also allow the accommodation of the viscoplasticity and concomitant wall slip behavior of energetic suspensions (1-4). The challenges associated with rheological characterization of energetic formulations and ramifications of the rheology data collected on the safety and the quality of energetic materials are available elsewhere (5). Here one of the most important methodologies for the rheological characterization of energetic suspensions, i.e., on-line and off-line slit die rheometers with continuously adjustable gap change mechanisms, will be covered. First the working principles will be described, second the hardware will be reviewed and finally some typical data on a LOVA propellant will be presented to illustrate the working principles of the rheometers.

The rheological characterization of the energetic formulations in the relatively large shear rate range, i.e., typically greater than 1 s^{-1} , can be carried out either using capillary or rectangular slit dies. In such characterization the flow rate is generally altered as the fully developed pressure gradient is determined at constant temperature. For the capillary flow only the total pressure drop can be measured and thus to determine the fully-developed pressure gradient, corrections for the pressure drops associated with the entry and exit flows need to be carried out. For capillary flow this is achieved by using a series of capillaries with systematically varied length over diameter ratios at constant capillary diameter. However, considering that the wall slip correction also requires changes in the capillary dimensions, i.e., changing the diameter systematically at constant length over the diameter ratio, the resulting procedures are very labor-intensive (6-8). On the other hand the slit die has an inherent advantage in that pressure transducers can be installed

flush with the surface of the slit die to enable the direct determination of the pressure distribution and hence the fully-developed pressure gradient in the slit die for a given flow rate. However, the surface to volume ratio of the slit die needs to be altered systematically to allow the determination of the wall slip velocity and thus enabling the correction for the true shear rate at the wall to be made. In the following two slit rheometers particularly suited to the characterization of energetic materials are described, starting with the basic operating principle.

II. Working principles of adjustable-gap rheometer

Let us analyze the formation of a slip velocity at the two walls of a slit with a gap of $2B$ on the basis of an apparent slip layer with a thickness, δ . The apparent slip layer thickness is generally a function of the volume loading level (volume fraction, ϕ) of the rigid particles and the particle size average, D_p , and maximum packing fraction of the particles, ϕ_m , of the energetic formulation (9, 10). The slip layer thickness, δ , is given as a function of the particle mean diameter (harmonic mean), D_p , and the volume loading level, ϕ , over the maximum packing fraction of the particles of the energetic suspension, ϕ_m , i.e., ϕ/ϕ_m (9, 10):

$$\frac{\delta}{D_p} = 1 - \frac{\phi}{\phi_m}. \quad (1)$$

Although the equations for the velocity distributions, the flow rate versus the pressure drop relationship and the shear rate at the wall will be derived here for this apparent slip mechanism the equations are applicable to any type of wall slip mechanism (9). The behavior of the suspension is represented by a Herschel-Bulkley type viscoplastic constitutive equation (- sign is used for negative shear stress):

$$\tau_{yz} = \pm \tau_0 - m \left| \frac{dV_z}{dy} \right|^{n-1} \left(\frac{dV_z}{dy} \right) \quad (2a)$$

for the absolute value of the shear stress, $|\tau_{yz}| \geq \tau_0$, i.e., the yield stress of the suspension, and the shear rate $(dV_z/dy) = 0$ for $|\tau_{yz}| < \tau_0$. Here the shear rate sensitivity index, n , consistency index, m and the yield stress, τ_0 , are the parameters of the Herschel-Bulkley equation. The Ostwald-de Waele or “power law” behavior represents the behavior of the shear viscosity of the binder phase:

$$\tau_{yz} = -m_b \left| \frac{dV_z}{dy} \right|^{n_b-1} \left(\frac{dV_z}{dy} \right) \quad (2b)$$

where m_b and n_b are the consistency index and the power law index parameters of the Ostwald-de-Waele “power-law” equation.

Analysis of Rectangular Slit Flow:

The apparent slip mechanism for the axial flow of a viscoplastic fluid through a rectangular slit of width W , gap of $2B$ and length L (with $L \gg W \gg 2B$) under a constant pressure gradient of $\frac{dP}{dz}$ is considered. The velocity distributions for the three zones (I is the apparent slip layer, II is the deforming viscoplastic suspension and III is the plug flow region) are:

$$V_z^I = \left[\frac{-\partial P}{\partial z} \frac{B}{m_b} \right]^{s_b} \frac{B}{(s_b + 1)} \left[1 - \left(\frac{y}{B} \right)^{s_b + 1} \right] \quad \text{for } B \geq y \geq (B - \delta) \quad (3)$$

with slip velocity $U_s = V_z^I \Big|_{(B-\delta)}$

$$U_s = \frac{\tau_w^{s_b}}{m_b^{s_b}} \frac{B}{(s_b + 1)} \left[1 - \left(1 - \frac{\delta}{B} \right)^{s_b + 1} \right] \quad (4)$$

The use of Binomial Theorem with $\left(1 - \frac{\delta}{B} \right)^{s_b + 1} \cong 1 - \frac{\delta}{B} (s_b + 1)$ provides

$\beta = \frac{\delta}{m_b^{s_b}}$ and $U_s = \frac{\delta}{m_b^{s_b}} \tau_w^{s_b}$, where β , is Navier's slip coefficient. This is the same slip

velocity versus shear stress behavior obtained for other flows also, including the plane Couette flow and capillary flow (9). Obtaining the same Navier's slip coefficient, β , for both the drag flow based plane Couette flow and the pressure-driven capillary and rectangular slit flows is important. It justifies why wall slip data collected using steady torsional flow together with capillary rheometry should and do fall within the confines of a single wall-slip velocity versus wall shear stress curve (4, 7).

The velocity distribution for the deforming viscoplastic fluid in the rectangular slit is given as:

$$V_Z^{II} = U_s + \frac{B}{(s+1) \tau_w m^s} \left[\left(\tau_w \left(1 - \frac{\delta}{B} \right) - \tau_0 \right)^{s+1} - \left(\tau_w \frac{y}{B} - \tau_0 \right)^{s+1} \right] \quad \text{for } y_0 < y \leq (B-\delta) \quad (5)$$

where $\tau_w = \frac{-dP}{dz} B$. The velocity of the plug, V_Z^{III} , for $0 \leq y < y_0$ (where y_0 is the location

where the absolute value of the shear stress is equal to the yield stress) becomes:

$$V_Z^{III} = U_s + \frac{B}{(s+1) \tau_w m^s} \left(\tau_w \left(1 - \frac{\delta}{B} \right) - \tau_0 \right)^{s+1} \quad (6)$$

Upon the integration of the velocity distribution Equations 3-6, the volumetric flow rate Q (for $\delta \ll B$) is obtained:

$$Q = Q_S + \frac{2WB^2}{(s+1)\tau_w^2} \frac{(\tau_w - \tau_0)^{s+1}}{m^s} \frac{[\tau_w(s+1) + \tau_0]}{(s+2)} \quad (7)$$

where Q_S is the volumetric flow rate due to slip, i.e., $2BWU_S$. The classical volumetric flow rate versus the wall shear stress relationship for rectangular slit flow of Bingham fluid subject to no-slip at the wall is obtained from Equation 7 by setting $\delta=Q_S=0$ and $s=1$ as:

$$Q = \frac{2WB^2\tau_w}{3m} \left[1 - \frac{3\tau_0}{2\tau_w} + \frac{1}{2} \left(\frac{\tau_0}{\tau_w} \right)^3 \right]. \quad (8)$$

How can the slip velocity values be obtained from the flow curves of rectangular slit flow in which the gap of the rectangular slit, $2B$, is systematically changed and the corresponding flow rate versus the shear stress data are collected? The derivative of the apparent shear rate, $(3Q/(2WB^2))$ versus the reciprocal half-gap, $1/B$, at constant wall shear stress provides the wall-slip velocity for rectangular slit flow (11):

$$\left. \frac{d\left(\frac{3Q}{2WB^2}\right)}{d(1/B)} \right|_{\tau_w} = 3U_S(\tau_w) \quad (9)$$

The true deformation rate of the suspension, $\dot{\gamma}_W$, at the interface between zones I and II, i.e., at $(y=B-\delta)$ can be determined from Equation 5 as:

$$\left. \frac{-dV_Z}{dy} \right|_{y=B-\delta} = \dot{\gamma}_w = \frac{(Q-Q_s)}{2WB^2} \left[2 + \frac{d \ln(Q-Q_s)}{d \ln \tau_w} \right] \quad (10)$$

for $\delta \ll B$. Equations 9 and 10 can also be directly obtained from the integration of the velocity distribution without assuming a constitutive behavior to the bulk fluid as shown below:

$$V_Z = U_s + \int_y^B \dot{\gamma} dy \quad (11)$$

Integrating by parts gives:

$$\left[\frac{Q-Q_s}{2WB^2} \right] = \frac{1}{\tau_w^2} \int_0^{\tau_w} \dot{\gamma} \tau_{zy} d\tau_{zy} \quad (12)$$

Taking the derivative of Equation 12 with respect to the wall shear stress, τ_w , and the use of the Leibniz formula for differentiating an integral provide again Equation 10 for the slip corrected shear rate at the wall, $\dot{\gamma}_w$ for axial flow in a rectangular slit under fully-developed flow conditions.

In the characterization of the volumetric flow rate versus the wall shear stress behavior of viscoplastic energetic formulations under systematic changes of the surface-to-volume ratio of the slit ($1/B$) the use of a slit die rheometer with a continuously adjustable gap is thus particularly advantageous (11, 12). If the gap and the flow rate can be independently varied both the slip velocity (from Equation 9) and the slip-corrected wall shear rate (from Equation 10) can be obtained.

Let us continue to probe the effect of wall slip on the development of the flow curve by considering the relationship between the relative viscosity, η_r (suspension viscosity over the shear viscosity of the binder) and $\frac{\phi}{\phi_m}$ (using the Krieger and Dougherty relationship [13]):

$$\eta_r = \left(1 - \frac{\phi}{\phi_m}\right)^{-2.0} \quad (13)$$

Typical results for a suspension with a Newtonian shear viscosity and with a Newtonian binder are shown in Figure 1 which indicates that with increasing gap, i.e., decreasing surface to volume ratio of the rheometer, pressure drop and hence the wall shear stress, τ_w , increase at constant apparent shear rate (direct consequence of the change in the surface to volume ratio of the rheometer). Figure 2 indicates that the effect of wall slip is governed by the slit gap, B over the particle radius, a, i.e., B/a ratio. The effect of wall slip becomes negligible for relatively large values of the B/a and for low values of $\frac{\phi}{\phi_m}$.

Thus, the objective of the adjustable gap rheometer is to generate different surface to volume ratios of the die to allow the determination and the characterization of the wall slip effect. The adjustable gap rheometer is described next.

III. Description of the On-line and Off-line Slit Rheometer with Continuously adjustable Gap and Procedures to Follow

The adjustable gap slit rheometer can be used in the on-line, or in the off-line mode. In the on-line (or in-line) mode the rheometer is connected to a processor (Figure 3). In both modes, this rheometer consists of a slit die with a movable plate, which allows the gap separation, 2B, between the two plates to change. As shown in Figure 3, the

rheometer is equipped with a series of equally spaced pressure and temperature sensors, which are installed flush with the inner surface of the rheometer. The gap adjustment mechanism is generally coupled to a remotely controllable stepper motor (3, 14).

The on-line rheometer typically is connected to a single and twin screw extruder or a gear pump (Figure 4). If an extruder is used to deliver the energetic suspension to the rheometer, the extruder is starve-fed. The starve-feeding is accomplished by the use of a gravimetric or loss-in-weight feeder which feeds the extruder at a constant volume flow rate, Q . The extruder has multiple feeding ports and multiple feeders to allow complete formulations to be processed and prepared prior to the characterization.

In the off-line mode the rheometer contains a reservoir that needs to be pressurized with the action of a ram (Figure 5). For energetic materials it is very important to:

1. Fill the reservoir with the energetic material under conditions that are safe. The usual methodologies used for polymers and other inert materials including suspensions in conventional slit or capillary rheometry involve the tamping of the materials into the reservoir using, typically, a tamping rod. Obviously tamping is not acceptable with energetic materials. Thus, the rheometer for energetic characterization applications should have the facility for the reservoir to be filled remotely (14).
2. Second, the entrainment of air into energetics, not only affects the wall slip and the rheological behavior of the energetic suspension, but is also a safety concern: very high localized temperatures are theoretically possible due to adiabatic compression of entrained air bubbles. Thus, the reservoir of the rheometer needs to be filled under vacuum.

These two requirements can be achieved using the filling station and a specialized cartridge, which serves as the reservoir of the rheometer as shown in Figure 5 (14). The filling station (Figure 5a) allows the cartridge to be filled under vacuum and at constant temperature and under remote control, followed by the sealing of the cartridge with a ram attachment for the slit rheometer. After sealing, the cartridge can be thermostatted to allow the energetic material to reach the desired temperature, followed by placement of the cartridge into the slit rheometer (Figure 5). Upon the installation of the cartridge into the rheometer the ram is moved at desired speeds allowing the flow rate, Q , to be changed while the pressure distribution is measured. The use of Equations 9 and 10 then allows the determination of the wall slip velocity at each shear stress and corrections of the wall shear rate.

Thus, for both the off-line and the on-line slit rheometer the procedure is as follows:

1. Run the rheometer at different flow rates and collect the corresponding pressure distribution
2. Determine the fully developed region of the pressure distribution, i.e., the fully developed pressure gradient, dP/dz for each flow rate.
3. This provides the wall shear stress at each flow rate, $\tau_w = B dP/dz$.
4. Change the surface to volume ratio of the slit die by altering the gap of the rheometer, $2B$, and collect the corresponding wall shear stress versus the flow rate information.
5. Use Equation 9 to determine the slip velocity and Equation 10 to determine the slip corrected wall shear rate:

Thus, determination of wall shear stress, τ_w versus apparent shear rate behavior at multiple gap openings provides the data necessary to characterize the wall slip velocity as well as the slip corrected shear rate at the wall.

IV. Sample Results and Discussion

The typical pressure versus distance in the slit die data collected at different gap openings are shown in Figure 6 for a LOVA propellant (3). The data were analyzed first to determine if the pressure vs. distance data are linear. This is shown in Figure 6 for the solvent concentration of 13% by weight. The shear stress at the wall is obtained from the fully developed region, i.e., from the linear gradient of pressure vs. the distance. As shown in Figure 6 the data collected with all of the four transducers were in the linear pressure gradient (fully-developed flow condition) regime. This is evident from the relatively high values of the correlation coefficient R^2 , which approach 1.0 indicating a perfect linear regression. This is interesting and indicates that for the LOVA propellant investigated, the entry region to the die is indeed very short and the velocity and the temperature distribution reach their steady state distributions rapidly in the slit die rheometer.

The apparent shear rate versus the reciprocal gap as a function of wall shear stress behavior of the LOVA propellant at the solvent level of 13% by weight and at a temperature of 121 °F is shown in Figure 7 for the three different gaps used in the experiments. This combination is necessary to be able to carry out the wall slip corrections. The analysis of the data then followed equations 5-7. From the apparent shear rate vs. the reciprocal gap information collected at various shear stress values the slopes, which are equal to 6 times the slip velocity could be collected (Figure 7). The fit of the data as well as the typical correlation coefficients, R^2 , are shown in the same figure.

The wall slip velocities, determined from the slopes, are shown in Figure 8. The wall slip vs. the wall shear stress behavior is linear upholding the expectation that the binder with

the solvent (13%) behaves as a Newtonian material and that the temperature could be kept reasonably constant during the experiment due to the relatively low viscous energy dissipation expected- as also determined experimentally (3). The slope of the equation represents the Navier's wall slip coefficient, β , which is equal to the slip layer thickness, δ , divided by the shear viscosity of the pure binder, and the coefficient for the LOVA propellant (at the temperature and solvent concentration used) is equal to $3 \cdot 10^{-8}$ m/(Pa-s).

The volumetric flow rate due to slip i.e., $Q_s = U_s W H$ was determined for each condition and together with the corresponding volumetric flow rate value was used to determine the $\ln(Q-Q_s)/\ln \tau_w$ data. The true wall shear rate was determined according to Equation 10 and the corrected behavior is shown in Figure 9. The data at this temperature and solvent concentration are fitted with a Hershel-Bulkley type viscoplastic constitutive equation. The yield stress is around 75,000. Pa, the shear rate sensitivity index (power-law index, n) is 0.18 and the consistency index, m , is $4934 \text{ Pa-s}^{0.18}$.

V. Conclusions

The working principles of the adjustable gap rheometer and the typical hardware used (both on-line and off-line versions) are described. The adjustable gap rheometer is applicable to the characterization of energetic materials (explosion proof for safety and enabling the determination of wall slip and the yield stress of viscoplastic energetic suspensions). The methodologies used are outlined and sample data are presented, analyzed and discussed.

VI. References

1. M.A. Michienzi, C.M. Murphy, D. M. Kalyon and S. Railkar, "Wall Slip and Capillary Flow Behavior of Extrudable Composite Propellant", Proceedings of

- JANNAF Conference Propellant Development and Characterization Subcommittee Meeting, Sunnyvale, California (1997).
2. S. E. Prickett, D. M. Kalyon and S. Railkar, "Characterization of the Temperature-Dependent Shear Viscosity Material Function of AA-6 Propellant", Proceedings of JANNAF Conference Propellant Development and Characterization Subcommittee Meeting, Sunnyvale, California (1997).
 3. S. E. Prickett, D. Kalyon (SIT), J. E. Brough, S. G. Johnson, C. M. Murphy, and G. W. Thomas, "Use of an Adjustable-Gap On-Line Rheometer for the Characterization of the Wall Slip and Shear Viscosity Behavior of LOVA EX-99", Proceedings of the 30th JANNAF Propellant Development and Characterization Subcommittee Meeting. Colorado Springs (2002).
 4. D. M. Kalyon, P. Yaras, B. Aral and U. Yilmazer, "Rheological Behavior of a Concentrated Suspension: A Solid Rocket Fuel Simulant", J. Rheol., 37, 35-53 (1993).
 5. D. M. Kalyon, "An Overview of the Rheological Behavior and Characterization of Energetic Formulations: Ramifications on Safety and Product Quality", Journal of Energetic Materials, 24, 3, 213-246 (2006).
 6. M. Mooney, "Explicit Formulas for Slip and Fluidity", J. Rheol., 2, 210-222 (1931).
 7. U. Yilmazer and D. M. Kalyon, "Slip Effects in Capillary and Parallel Disk Torsional Flows of Highly Filled Suspensions", J. Rheol., 33, 1197-1212 (1989).
 8. Kalyon, D. M. and Yilmazer, U., "Rheological Behavior of Highly Filled Suspensions Which Exhibit Slip at the Wall", Polymer Rheology and Processing, A. Collyer and L. Utracki, eds., London: Elsevier Applied Science, 1990.
 9. D. Kalyon, "Apparent Slip and Viscoplasticity of Concentrated Suspensions", J. Rheol., 49, 621-640 (2005).
 10. P. Yaras, "Rheological Behavior and Twin Screw Extrusion Flow of Non-colloidal Concentrated Suspensions", PhD thesis, Stevens Institute of Technology, Hoboken, NJ, USA.
 11. D. M. Kalyon, H. Gokturk and I. Boz, "An Adjustable Gap In-Line Rheometer", Society of Plastics Engineers Annual Technical Conference, Toronto, Canada, May (1997).

12. D. M. Kalyon, H. S. Gokturk, "Adjustable Gap Rheometer", U.S. Patent and Trademark Office; # 5,277,058; issued on Jan. 11, 1994.
13. I. M. Krieger and T. J. Dougherty, "A mechanism for non-Newtonian flow in suspensions of rigid spheres", Transactions of Rheology, 3, 137-152 (1959).
14. <http://www.mprus.com>

List of figures:

1. Wall shear stress versus apparent shear rate for a Newtonian suspension with a Newtonian binder at different slit die gaps.
2. The effect of slip on the flow rate, i.e., volumetric flow rate due to slip, Q_s , over the total flow rate, Q , ratio (Q_s/Q) versus the volume fraction of particles, ϕ , at differing slit half-gap over the particle radius, B/a , ratios.
3. Working principle of the adjustable gap slit die.
4. On-line version of the adjustable gap slit rheometer (shown connected to a twin screw extruder).
5. Off-line version of the adjustable gap slit rheometer and filling station.
6. Pressure versus distance in the slit die for differing values of the slit gap for a LOVA propellant at 121 °F and 13% solvent (by weight).
7. Apparent shear rate versus reciprocal gap at various wall shear stress conditions for a LOVA propellant at 121 °F and 13% solvent (by weight).
8. Slip velocity versus wall shear stress behavior of a LOVA propellant at 121 °F and 13% solvent (by weight).
9. Flow curve (wall shear stress versus the slip corrected wall shear rate) of a LOVA propellant at 121 °F and 13% solvent (by weight)

Development of flow curves at $\phi=0.7$

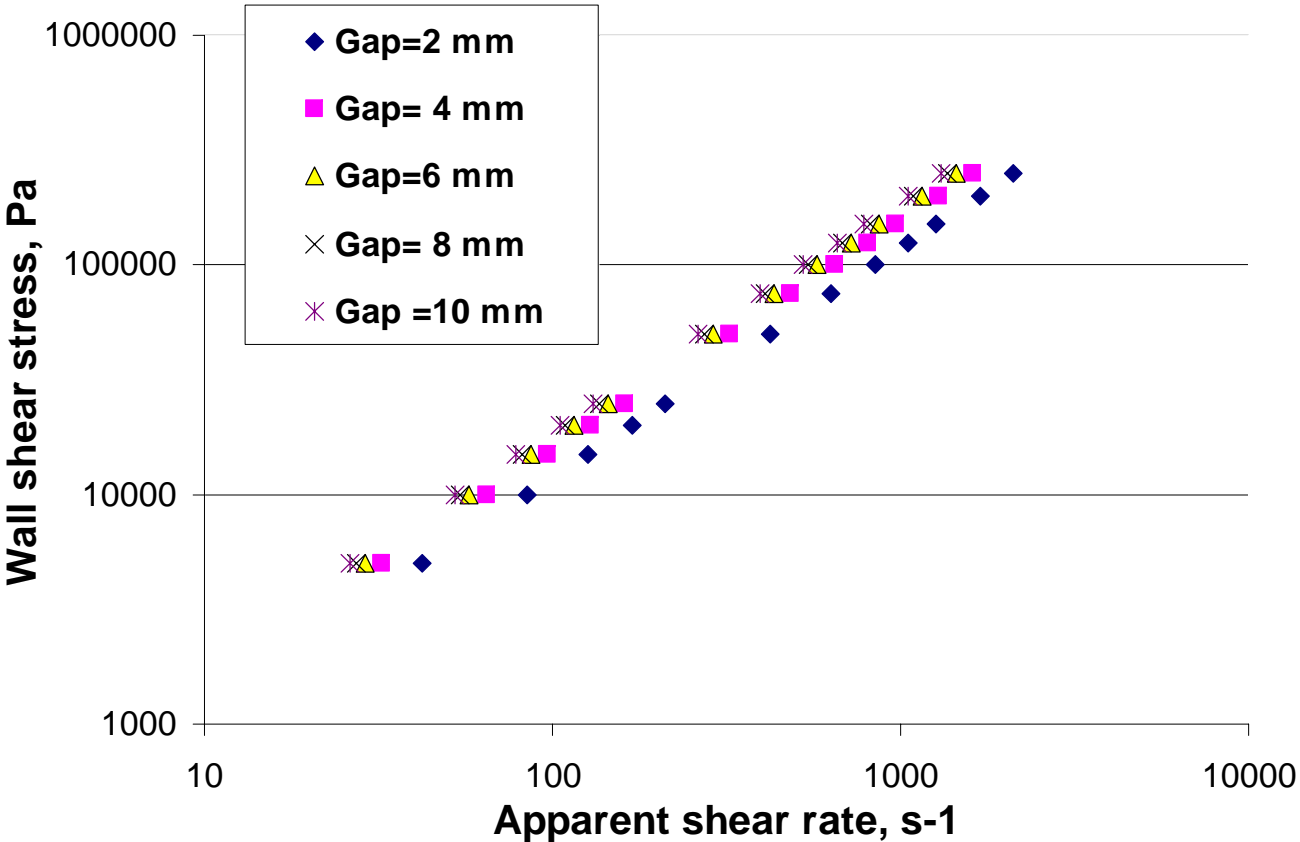


Figure 1

Q/Qs for different half-slit gap, B, over particle radius, a, ratios (B/a)

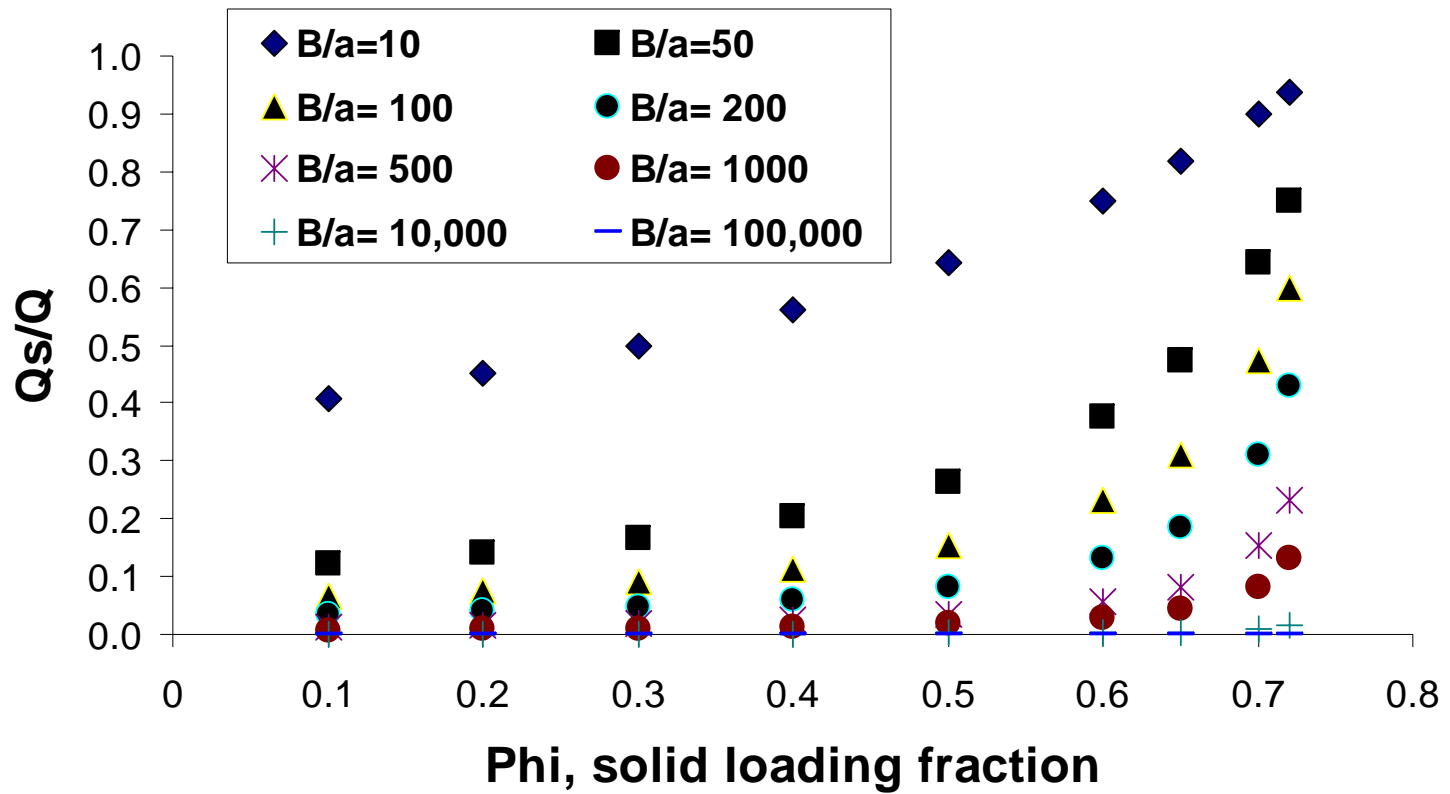
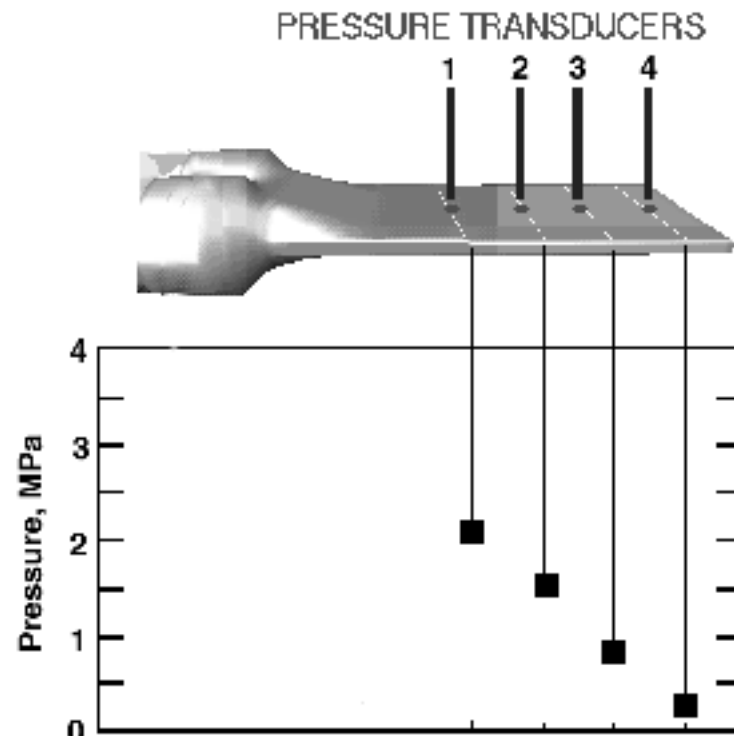


Figure 2

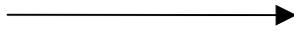
ADJUSTABLE GAP RHEOMETER



Pressure versus distance in the die

Figure 3

Twin screw
extruder



Adjustable gap slit die
rheometer

Figure 4

Off-line adjustable gap slit die

Filling station



Figure 5

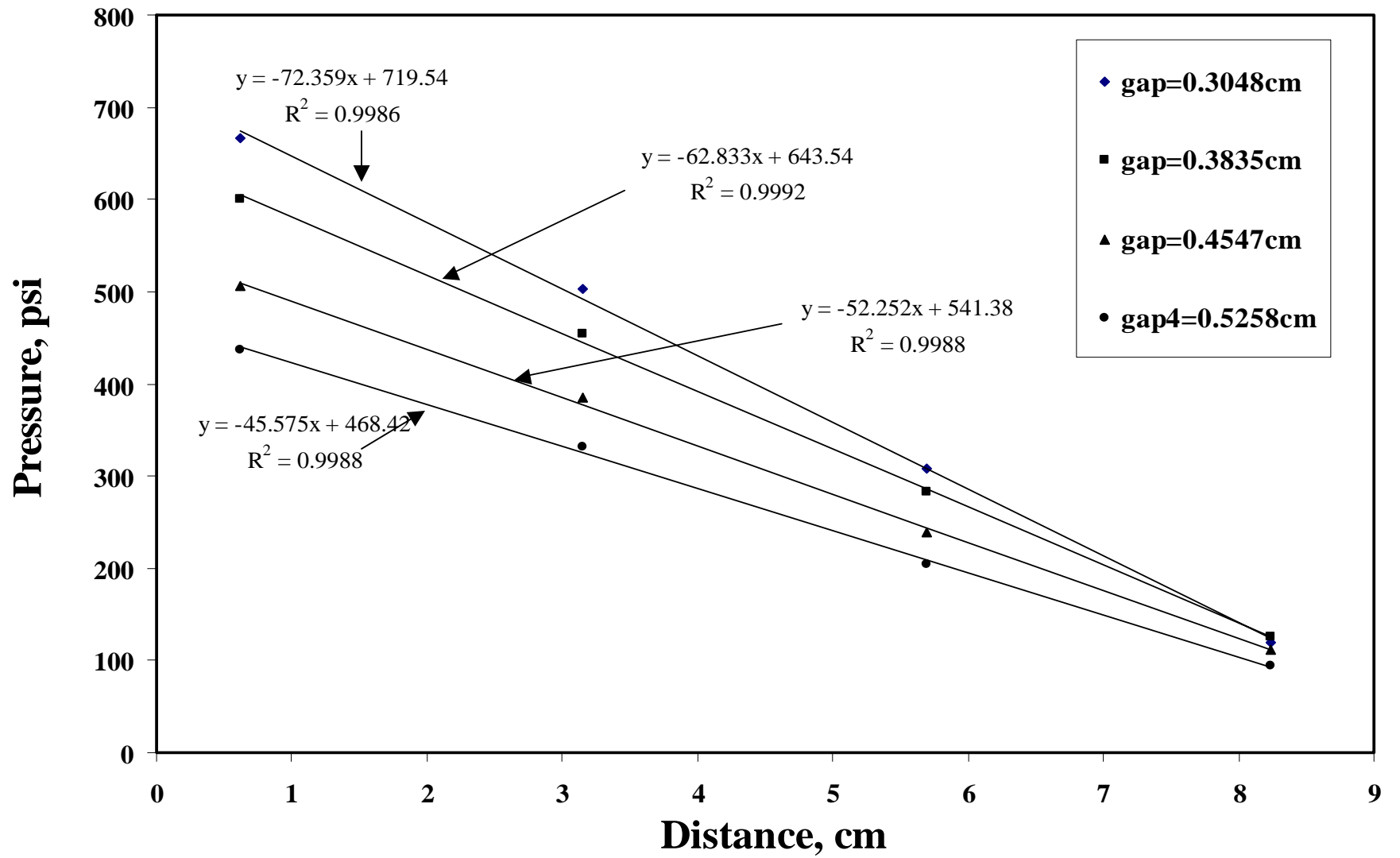


Figure 6

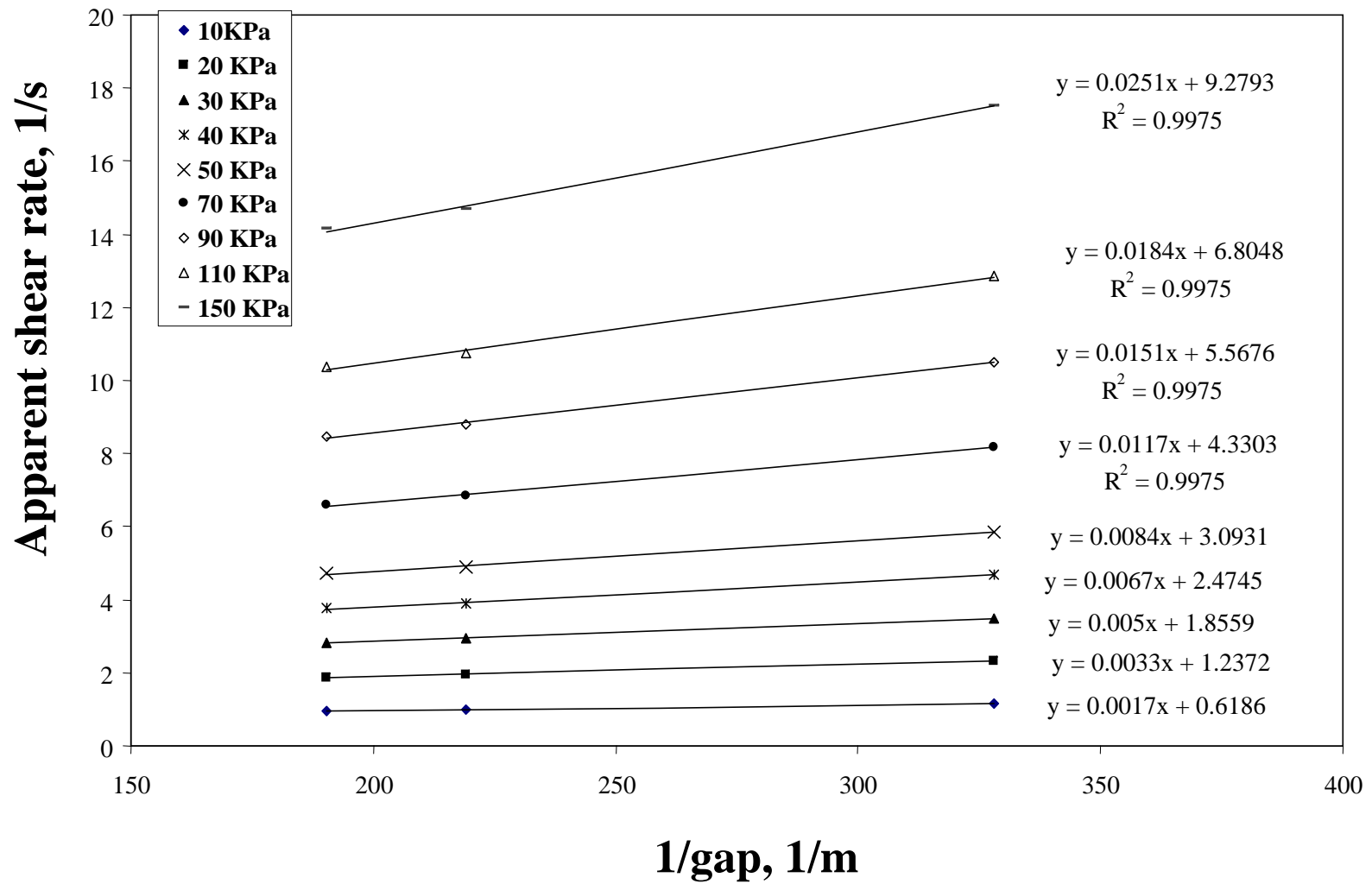


Figure 7

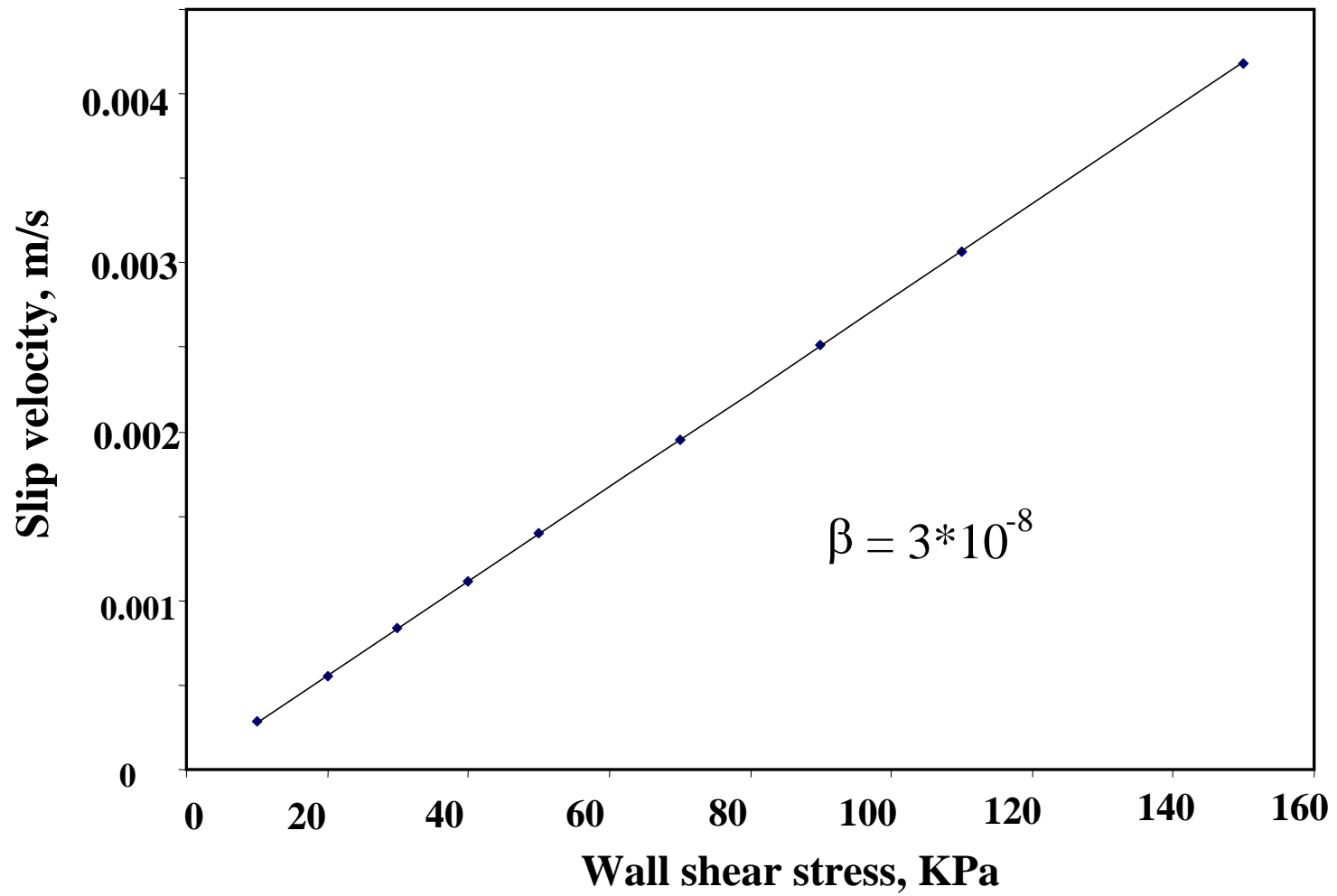


Figure 8

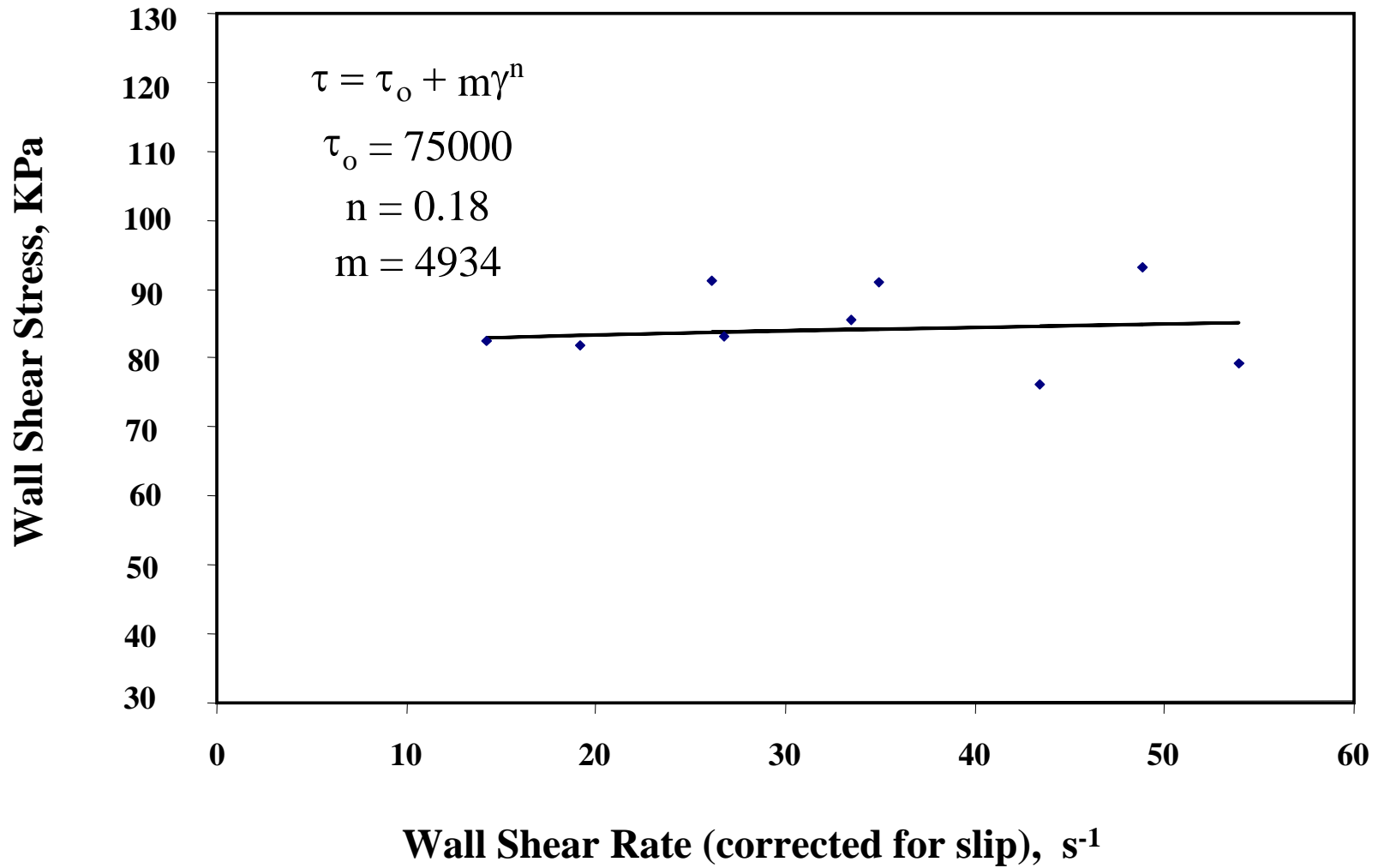


Figure 9